Eur. Phys. J. D **26**, 285–295 (2003)
DOI: 10.1140/epjd/e2003-00260-0

THE EUROPEAN PHYSICAL JOURNAL D

Generation of high-current electron beams by a hollow cathode with a ferroelectric plasma source

J.Z. Gleizer, A. Krokhmal, Ya.E. Krasik[a], and J. Felsteiner

Physics Department, Technion-Israel Institute of Technology, 32000 Haifa, Israel

Received 10 December 2002/ Received in final form 10 April 2003
Published online 12 August 2003 –

Abstract. This paper presents results and analysis of an experimental investigation of the operation of a hollow cathode (HC) with an incorporated ferroelectric plasma source (FPS). It was shown that the use of FPS based on a BaTi solid solution allows one to ignite and to sustain a 10^2–10^3 A HC discharge with duration of 10^{-3}–10^{-5} s at background pressure of $\sim 5 \times 10^{-3}$ Pa while keeping the HC design with small dimensions. It was found that the development of the HC discharge is accompanied by formation at the surface of the FPS of dense plasma which serves as a powerful (hundreds of kW) pulsed source of current carrying electrons. Parameters of the HC plasma (radial distribution of the plasma density and temperature and plasma potential) for different discharge current amplitudes and two types of FPS are presented. Application of the FPS as an electron source in a diode under an accelerating pulse $\leq$300 kV and pulse duration $\leq$400 ns showed that the latter operates in a plasma pre-filled mode with a current amplitude up to 1.6 kA. Parameters of the diode and electron beam for different experimental conditions are presented and discussed.

PACS. 52.50.Dg Plasma sources – 29.25.Bx Electron sources – 52.25.Tx Emission, absorption, and scattering of particles

1 Introduction

There is a continuous interest in electron sources which can be used for the generation of high-current pulsed electron beams [1,2]. This interest has stimulated a variety of experiments which can be conventionally separated into two groups, namely experiments on passive and active plasma cathodes. By passive cathodes we mean here cathodes in which a plasma is produced by an accelerating pulse, *i.e.* explosive emission or surface flashover plasma [3]. Contrary to passive cathodes, in active cathodes a plasma is produced by an external source prior to the application of the accelerating pulse (ferroelectric plasma cathodes [4], hollow cathode and hollow anode plasma sources [5]). Therefore, these types of cathodes do not depend on the parameters of the accelerating pulse.

The commonly used explosive emission plasma cathodes show excellent performance at a high electric field ($E > 10^7$ V/cm) with a fast rise time [$\mathrm{d}E/\mathrm{d}t > 10^{13}$ V/(cm s)] and a short pulse duration ($<10^{-7}$ s) [3]. However, at lower electric fields and slower rise times there is a significant time delay in the formation of an explosive plasma and it has poor uniformity [3,6]. In addition, this explosive emission plasma limits the duration of the accelerating pulse because of the fast plasma expansion velocity that leads to shortening of the accelerating gap [3].

Recently, several experimental investigations were devoted to carbon fiber and velvet made cathodes [6–8]. These cathodes showed significantly lower threshold for the electric field which is required for the formation of the plasma, $E_{\mathrm{th}} \leq 10^4$ V/cm and a slower plasma expansion velocity ($<10^6$ cm/s). However, it was shown that these cathodes produce electron beams with a relatively large divergence [6]. Also, the temporal behavior of the electron beam current amplitude was characterized by sporadic high-frequency spikes [6]. These spikes are related to the spatial and temporal behavior of the cathode plasma [3].

Concerning active plasma cathodes, recent research has shown that ferroelectric plasma cathodes could be considered as promising candidates for the generation of high-current electron beams with satisfactory current density uniformity and large cross-sectional area [4,9]. However, additional research is needed in order to achieve generation of electron beams with current density $\geq$10 A/cm^2 without pre-filling of the diode by the plasma produced by the ferroelectric cathode [10]. Also, it is still questionable how really long is the lifetime ($\geq 10^6$ pulses) of this type of plasma cathodes.

Another type of active plasma sources is the hollow cathode (HC) which has important advantages compared with other types of plasma cathodes [4]. Indeed, it was shown that the HC can produce a plasma with a density of 10^{12} cm^{-3} and an emitting area of several tens

[a] e-mail: fnkrasik@physics.technion.ac.il

of cm^2 that is sufficient for the production of electron beams with current amplitudes up to several hundreds of A [4,11–14]. Let us note that the amplitude of the extracted electron beam current can reach the amplitude of the discharge current if electrons are emitted from the open plasma boundary [4,11]. Also, HC plasma sources are simple to operate and have a practically infinite lifetime. However, in order to achieve a high-current HC discharge ($I_{HC} > 100$ A) one has to keep high background gas pressure ∼0.1–1 Pa and to have a large ratio between the cathode and anode areas [11]. The latter is necessary in order to avoid arcing inside the HC cavity because of the increase of the plasma potential with respect to the HC and the anode when one increases the discharge current amplitude while keeping the ratio between the cathode and the anode areas unchanged. Also, the increase of the gas pressure results in a breakdown inside the accelerating gap. In order to avoid the increase of the pressure a gas puff valve was used that allows one to achieve a sharp gas pressure gradient between the HC and the accelerating gap [12,14]. However, implementation of a gas valve limits the lifetime and the repetition rate operation of the HC. For a high-current HC discharge at low-pressure (10^{-2}–10^{-3} Pa) a thermionic cathode was used with a heating power supply of several kW [13]. Nevertheless, even such a powerful thermionic cathode provides only $I_{HC} \leq 200$ A.

Recently we reported briefly the main results of the operation of a HC and a ferroelectric plasma source (FPS) incorporated in it and the use of this electron source in a high-voltage diode for generation of high-current electron beams [15]. It was found that the FPS effectively ignites and sustains high-current HC discharge at a relatively low background pressure. Also, it was shown that the application of the FPS allows one to operate with a HC having significantly smaller dimensions. Successful generation of electron beams with current amplitude up to 1.6 kA, electron energy of 300 keV and pulse duration of 300 ns was demonstrated as well. In this paper we describe in detail the same experiments with an emphasis on our investigation of the parameters of the HC plasma and the generated electron beam. For comparison, we also describe briefly our experiments with the same HC being ignited by spark discharges.

2 Experimental setup and diagnostics

The experimental setups used are presented in Figures 1a and 1b. In the experiments, we used a HC made in the form of a stainless steel cylinder, 290 mm in length and either 246 mm or 180 mm in diameter. The output window of the HC had a diameter of 120 mm. An output grid with an area of $S_g = 113$ cm^2 was placed in a 20 mm thick Plexiglas insulator. The grid was connected electrically to the cathode *via* a 1 kΩ resistor. We used anode grids with geometrical transparencies of 50% or 80% and grid cell sizes of 51 μm × 51 μm and 235 μm × 235 μm, respectively. The HC discharge was sustained by a pulse forming network (PFN) generator (10 kV, 5 Ω, 10 μs).

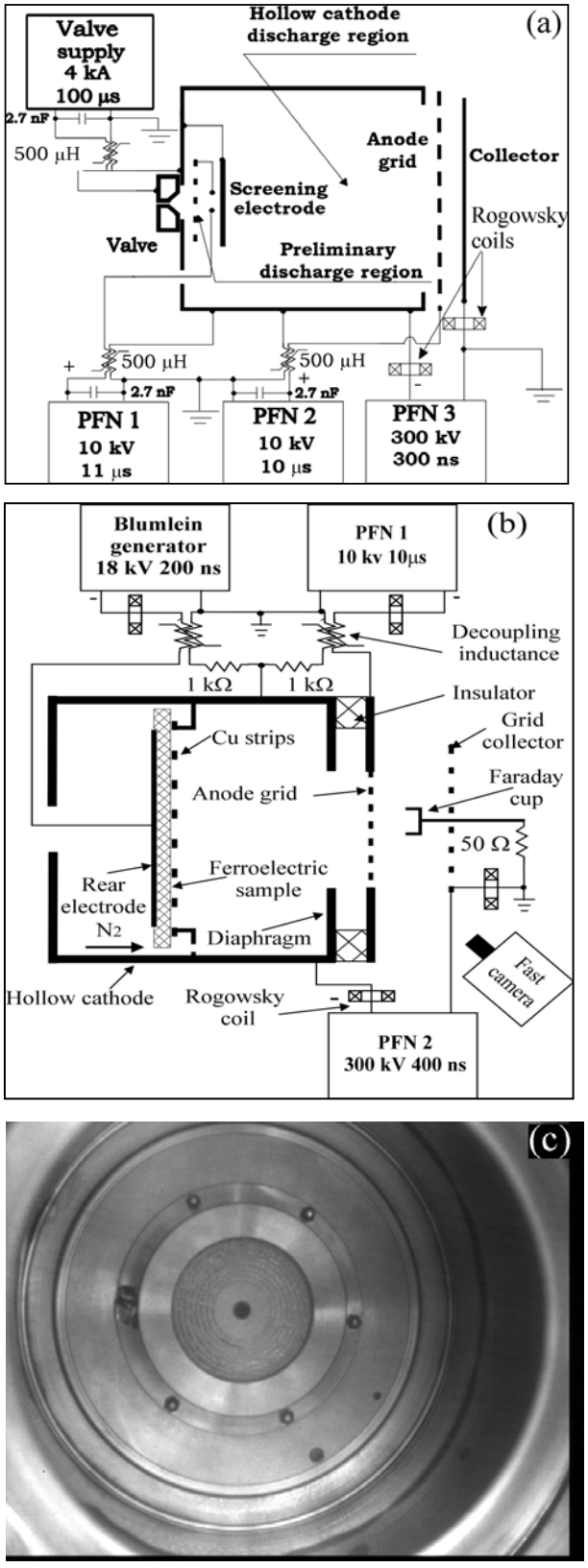

Fig. 1. (a) Experimental setup of the HC with the spark gap igniter; (b) experimental setup of the HC with the 154 cm^2 FPS; (c) an external top view of the HC with a 35 cm^2 FPS at the bottom.

The HC was placed inside a vacuum chamber, 500 mm in diameter and 900 mm in length. To inject gas we used either a gas puff valve or an adjustable gas flow. In these experiments we used N_2 gas. In the case of the gas puff valve the latter was installed at the back flange of the HC. The operation of the valve is described in reference [14]. The adjustable gas injection inside the HC was achieved through three holes symmetrically distributed in the bottom of the cathode cylinder. The vacuum in the chamber was kept by two turbo-molecular pumps (pumping rates of 500 l/s and 350 l/s) in the range of 1.3×10^{-2}–6.6×10^{-2} Pa, depending on experimental conditions.

In order to measure the gas pressure inside the HC and inside the accelerating gap we used a specially designed Penning probe. To produce a dc Penning discharge we used a positive bias voltage of 0.8–1.2 kV applied to the anode and a pair of Sm-Co magnets. The Penning probe was calibrated under stationary conditions according to the data obtained from an Edwards AIM-X-NW25 gauge by varying the vacuum in the chamber.

The parameters of the plasma (density, temperature, and ion energy) inside and outside the HC were estimated using double floating probes and biased collimated Faraday cups with and without transverse magnetic field. The diode voltage φ_c was measured by an active voltage divider. Two self-integrated Rogowsky coils (RCs) were used to measure the HC and collector currents (see Figs. 1a and 1b). The use of two RCs allowed us to account for possible electron losses in the HC holder.

A 4Quik05A fast framing camera was used to observe the light emission from the HC and from the accelerating gap. We also performed photography of the light emission by using narrow band filters ($\Delta\lambda = 8$ Å) for the H_α and H_β lines. By changing the time delay between the beginning of the gating pulse of the camera and the start of the HC discharge current or the accelerating pulse we obtained a set of framing photographs of the emitted light.

In the experiments of electron beam generation in a planar diode, a 12-stage high-voltage (HV) PFN generator was used with an output voltage $\varphi_{ac} \leq 300$ kV and pulse duration ≤ 400 ns [9]. A diode collector was made either of a high-transparency stainless steel grid or a Ta foil or a stainless steel disk with a thickness of 5 mm depending on the used diagnostics. The distance d_{ac} between the HC anode grid and the collector was varied in the range of 3–5 cm.

The uniformity of the electron beam was checked by X-ray imaging of the collector. In order to increase the X-ray output, we used a Ta foil collector with a thickness of 125 μm. The image produced on a screen (Ga_2O_2S:Tb, thickness of 200 $\mu g/cm^2$) placed on the back side of the Ta foil collector was obtained by the 4Quik05A camera. Let us note that we were able to observe space-resolved X-ray images because of the slow decay (several hundreds of μs) of the excited centers in the screen.

In the first experiments, in order to initiate the HC discharge we used ignition schemes based on different spark discharges. A spark discharge was ignited by a PFN generator (10 kV, 10 Ω, 11 μs). The fast gas puff valve provides a sharp pressure gradient between the cathode cavity and the accelerating gap (see Fig. 1a). However, these ignition schemes showed severe disadvantages. The main disadvantages are the limited lifetime of the spark igniters, the non-reproducibility of the HC discharge and the appearance of plasma spots at the surfaces of the HC and the HC anode grid at a discharge current amplitude $\geq$600 A. These plasma spots cause non-uniform plasma density distribution inside the HC and, respectively, non-uniform current density distribution of the extracted electron beam. Only the application of an additional screening electrode, which was placed at a distance of 2 cm from the spark gap, allowed us to partially solve these problems. Namely, we succeeded in operating the HC without plasma spot formation with a 1 kA discharge current amplitude and 10 μs pulse duration at a N_2 background pressure of $\sim(2\text{–}3)\times10^{-2}$ Pa inside the accelerating gap. With this screening electrode we obtained an almost uniform cross-sectional pressure distribution for each axial position inside the HC (see Fig. 2). Also, the background pressure inside the accelerating gap did not exceed 3×10^{-2} Pa which is acceptable for a diode operation with several hundreds of nanosecond duration accelerating pulse. Typical waveforms of the spark-gap current and HC discharge voltage and current are presented in Figure 3. It was found that

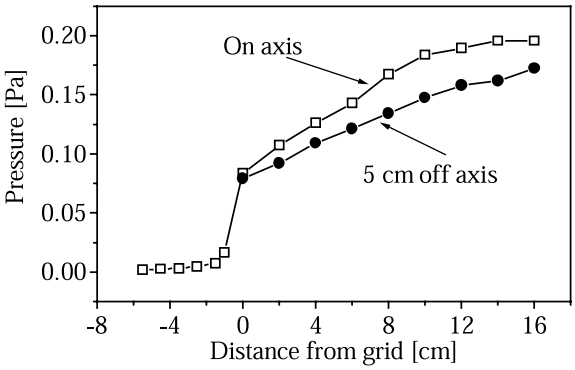

Fig. 2. The pressure distribution inside the HC with the spark gap igniter and inside the accelerating gap with the screening electrode at a time delay of $\tau_d \approx 775$ μs with respect to the beginning of the gas puff valve operation.

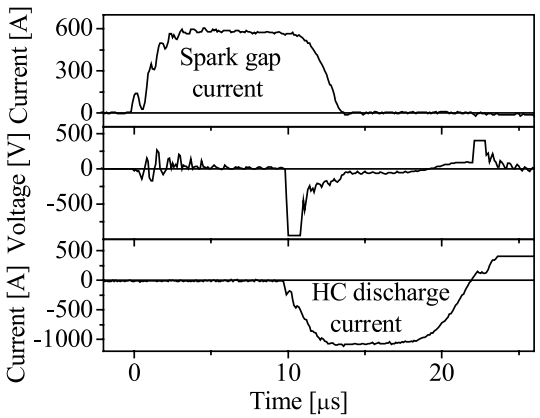

Fig. 3. Typical waveforms of the spark gap current, HC voltage and HC current. $\tau_d \approx 775$ μs.

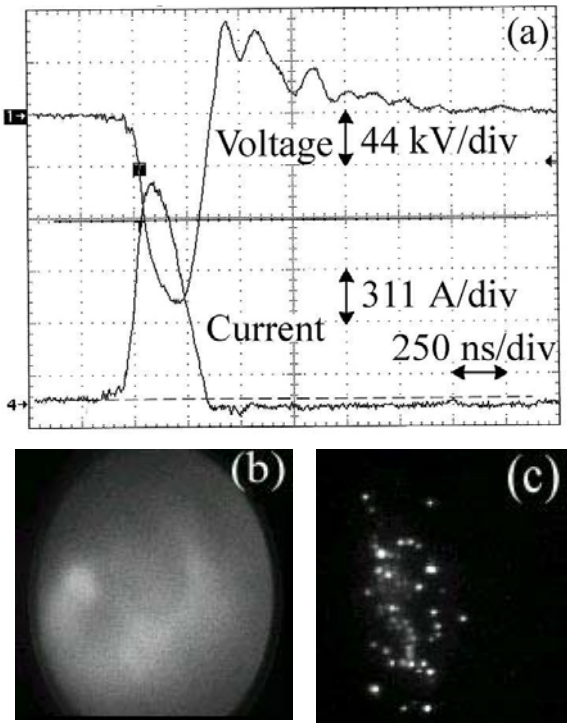

Fig. 4. (a) Typical waveforms of the diode voltage and current. The amplitude of the HC discharge current is 1 kA. Time delay between the beginning of the accelerating pulse and the beginning of the HC discharge current is 2 μs. (b) A framing photograph of the light emission from the HC operating with a fast gas puff valve and a screening electrode. Frame duration is 50 ns. (c) Typical framing photograph of plasma spots formation at the HC anode grid.

a time delay of $\sim$10 μs is required for the beginning of the main HC discharge with respect to the ignition of the spark gap discharge. During this time the plasma produced by the spark gap discharge expands and fills the cathode cavity. It was found that main HC cathode discharge (the amplitude of the discharge current up to 1 kA) is characterized by a potential drop of 100 ± 20 V which is typical for HC high-current discharges [5,14]. Also, we obtained satisfactory uniform light emission from the HC that indicates an almost uniform plasma density distribution. Applying an accelerating pulse of 150 kV amplitude allowed us to extract an electron beam with current amplitude up to 1.2 kA, 300 ns pulse duration (see Fig. 4a) and satisfactory electron density radial distribution (see Fig. 4b). However, the operation of the HC was not reproducible and reliable. Very often we obtained a constriction of the HC discharge or formation of plasma spots at the HC output grid during the HC discharge (see Fig. 4c). These plasma spots lead to shortening of the accelerating gap because of fast expansion of dense plasma.

In order to improve the reproducibility and reliability of the HC discharge ignition it was decided to use a FPS which can produce a uniform preliminary plasma [4,15]. Indeed, this surface discharge plasma which is generated by a driving pulse can be used as an efficient source of initial electrons [4,16,17] instead of a thermionic cathode [13] or spark gaps. In the first design of the HC with an incorporated FPS the latter was placed at the bottom of the HC cavity (see Fig. 1b). An external top view of the HC with the incorporated FPS is presented in Figure 1c. We tested the ignition and operation of the HC with two BaTi-based samples (thickness of $\sim$7 mm) having a plasma emitting surface of $\sim$35 cm^2 and $\sim$154 cm^2. Surface discharge was ignited by HV negative driving pulse with an amplitude $\leq$18 kV, rise time of $\sim$100 ns and pulse duration of $\sim$400 ns produced by the PFN1 generator and applied to the rear electrode of the FPS. The design of the FPS and its driving circuit are described in reference [15]. Here we note only that we tested the FPS with an output grid placed at the 3 mm from the ferroelectric front surface and also without an output grid. We did not obtain any difference in the ignition of the HC discharge when the FPS was operated without this grid or with grid having a 70% geometrical transparency. However, a significant worsening of the reproducibility in the ignition of the HC discharge was obtained when we used a grid with 55% transparency. Also, the application of a positive driving pulse causes the same effect of worsening in the HC discharge ignition. This can be explained by the smaller density of the surface plasma produced by a positive driving pulse as compared to a negative driving pulse [4,16,17].

3 Experimental results

3.1 Neutral density distribution inside the HC cavity and the accelerating gap

In order to achieve a high-current HC discharge one has to keep a relatively high background pressure inside the HC ($P = 0.1$–1 Pa) while at the same time to keep a relatively low background pressure inside the accelerating gap ($P \sim 10^{-2}$ Pa). Therefore, the measurements of the gas flow parameters were very important in our experiments. We performed measurements of the gas pressure distribution inside the HC and inside the accelerating gap for two cases. Namely, for the case of adjustable gas supply and for the case when we used a constant gas supply with a smaller adjustable gas flow together with the fast gas puff valve. In the first case the pressure inside the accelerating gap was $\sim 2.4 \times 10^{-2}$ Pa and in the second case $\sim 1.9 \times 10^{-2}$ Pa. Typical waveforms of the current driving the fast gas puff valve and the pressure build-up at a distance of 2 cm from the HC anode grid are presented in Figure 5a. Taking into account these data we applied the driving pulse to the FPS at a time delay of $\sim$775 μs with respect to the beginning of the current pulse (see Fig. 5a). Similarly to the case of the spark gap ignition, we obtained a satisfactory uniform cross-sectional pressure distribution for each axial position inside the HC (see Fig. 5b). Also, as expected, there is a fast decrease in the pressure towards to the HC anode grid. In the case of the constant gas flow the pressure inside the HC was $\sim 6.7 \times 10^{-2}$ Pa without a significant gradient inside the HC cavity and $\sim 2.4 \times 10^{-2}$ Pa inside

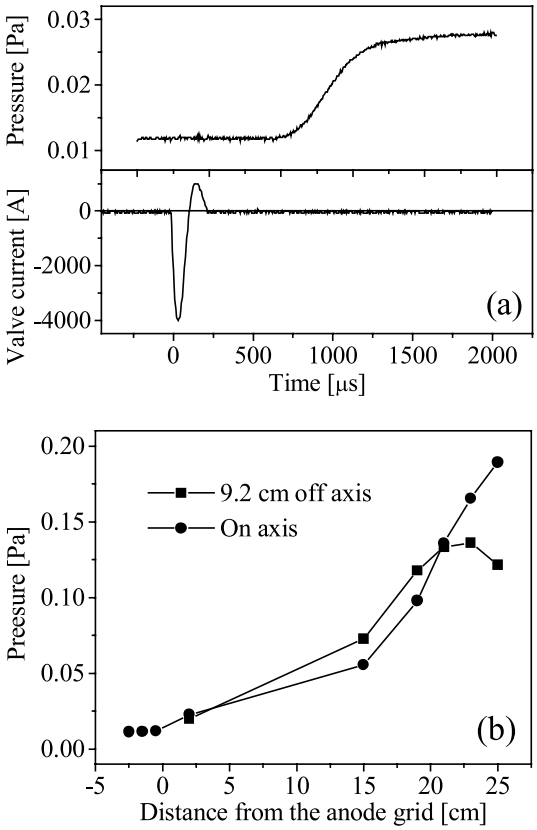

Fig. 5. (a) Typical waveforms of the gas puff valve current and the Penning probe pressure build-up. The Penning probe is placed inside the accelerating gap at a distance of 2 cm from the HC anode grid. (b) The pressure distribution inside the HC with a 35 cm^2 FPS and inside the accelerating gap with the screening electrode at $\tau_d \approx 775$ μs with respect to the beginning of the gas puff valve operation.

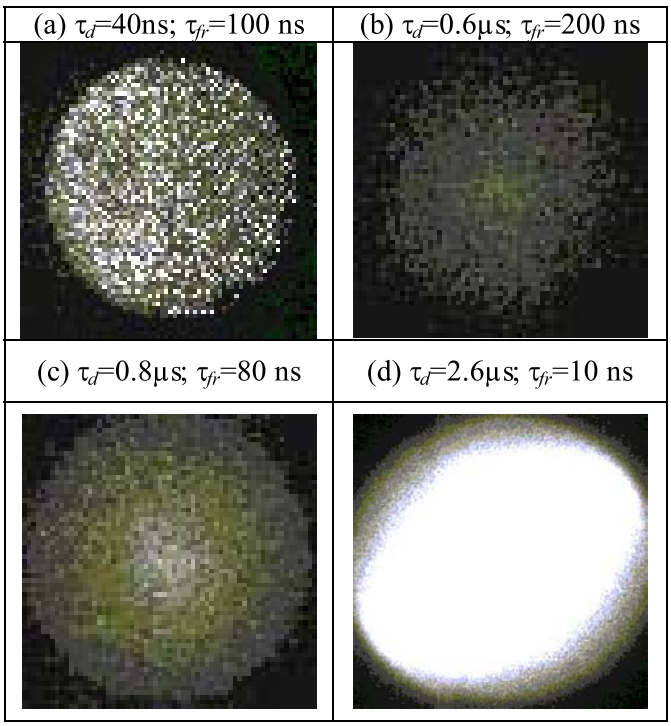

Fig. 6. A set of framing photographs of the 154 cm^2 FPS surface at different time delays τ from the beginning of the driving pulse and different frame durations τ_{fr}. The HC discharge pulse is applied with $\tau \cong 0.4$ μs. Here τ is the time delay of the frame beginning with respect to the beginning of the HC discharge, τ_{fr} is the frame duration. The amplitude of the HC discharge current is $I_d = 1.3$ kA.

the accelerating gap at a distance of 1 cm from the HC output grid.

3.2 Parameters of the FPS

The obtained framing photographs of the light emission from the surface discharge plasma were similar to those presented in our earlier publications [16,17]. Namely, it was found that the application of the driving pulse leads to almost simultaneous appearance of the light emission from the surface plasma with an approximately microsecond time scale decay of its intensity. In Figure 6a we present fast framing photographs of the light emission from the 154 cm^2 FPS prior to the HC discharge. Here we operated with a constant flow of N_2 gas. One can see a large amount of non-complete surface discharges. Similar photographs were obtained with the smaller area FPS [15]. Let us note that in the present experiment the FPS operates at a significantly larger background pressure compared with the earlier experiments [4,16,17]. In fact, the larger pressure can improve the uniformity of the surface discharge and decrease the erosion of the ferroelectric surface. The latter can be explained by the fact that the discharge occurs at the vicinity of the ferroelectric surface due to the ionization of gas atoms and molecules.

We also measured the parameters of the charged particle flows emitted from the surface plasma under the application of either a positive or a negative driving pulse with an amplitude of 18 kV to the rear electrode of the FPS. Similarly to our previous measurements [10,18], it was shown that the FPS emits fast and slow plasma flows. Typical waveforms of the driving pulse current and the electron current density measured by a biased collimated Faraday cup (CFC) at a distance of 1 cm from the FPS with the 35 cm^2 emitting area are presented in Figure 7. Similar results were obtained for the 154 cm^2 emitting area FPS. One can see that with a negative driving pulse charged particle flows are generated with almost double intensity as compared with a positive driving pulse. Therefore, in the experiments we operated with a negative driving pulse. The data concerning parameters of the plasma flows generated by the surface flashover were presented in references [10,15,18]. Here we summarize that the FPS emits electron and ion flows with current amplitudes up to 270 A and 15 A, respectively, with charged particle energy of several hundreds of eV, and pulse duration of several microseconds.

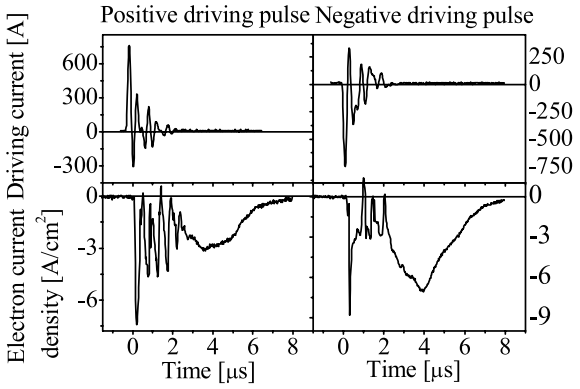

Fig. 7. Typical waveforms of the positive and negative driving pulses applied to the rear electrode of the 35 cm^2 FPS and of the electron current density obtained by a biased CFC placed at a distance of 1 cm from the front surface of the FPS.

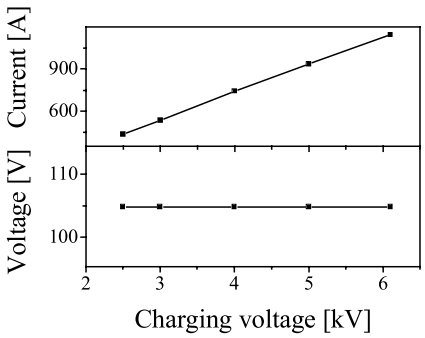

Fig. 8. Dependences of the HC discharge voltage and current amplitudes on the charging voltage of the HC power supply; $P = 2.4 \times 10^{-2}$ Pa, 35 cm^2 FPS.

3.3 Parameters of the HC discharge

The main HV pulse of the HC PFN generator was applied between the HC and the HC anode with a time delay of $\tau = 0.5$–3 μs with respect to the beginning of the driving pulse. The application of this HV pulse leads to the formation of a low-resistive high-current HC discharge. Namely, a linear dependence of the HC discharge current amplitude *versus* the charging voltage of the PFN2 generator was obtained (see Fig. 8). Also, it was found that the decrease of the pressure leads to an increase in τ. The dependence of τ *versus* the pressure and typical waveforms of the discharge current for different P is presented in our early publication [15]. The obtained increase of τ with the decrease of P was confirmed in our recent experiments with a HC and a 35 cm^2 FPS incorporated inside it in the millisecond time scale range and with an amplitude of the discharge current up to 900 A. Results of these experiments will be published elsewhere. Here we note that it was found that a further decrease in P up to $\sim 3 \times 10^{-3}$ Pa leads to the increase of τ to $\sim$20–30 μs. These data strongly indicate that the plasma density produced by the FPS is insufficient for the conduction of the main HC discharge current. Therefore, additional plasma formation by the ionization of the background gas is needed in order to form a high-current HC discharge.

In Figures 6b, 6c, and 6d we present fast framing photographs of the light emission from the 154 cm^2 FPS during the HC discharge. During the main HC discharge there is a significant increase in light emission from the FPS which presents a uniformly distributed light radiating area. A remarkable feature of this discharge is that it was achieved at a N_2 gas pressure of $\sim 6.7 \times 10^{-2}$ Pa and $I_{HC} \approx 1.2$ kA with a voltage drop between the HC and the anode of $\sim$100 V. A similar intense light emission from the FPS source was obtained at $\sim 3 \times 10^{-3}$ Pa and $I_{HC} \approx 0.8$ kA in a millisecond time scale of the HC discharge.

It was found that the obtained voltage drop between the HC and the HC anode does not depend on the amplitude of the HC discharge current (see Fig. 8). For instance, in the case of the 35 cm^2 FPS the increase of I_{HC} from 400 A to 1200 A does not affect the HC discharge voltage, *i.e.* the voltage stays at the same value of $\sim$100 V at a pressure of $\sim 6.7 \times 10^{-2}$ Pa. This can happen in the case when the HC plasma increases its density in order to conduct a current of a larger amplitude. Similar results were obtained for the HC operation with the FPS having a larger (154 cm^2) area. Namely, in the range of a HC discharge current amplitude of 400–1200 A (background pressure of $\sim 2 \times 10^{-2}$ Pa) the HC discharge voltage increases insignificantly, from 72 V to 80 V.

It also was found that the time duration of the HC discharge could be significantly increased. Namely, when we used a limiting resistor connected in series with the HC HV generator, the discharge duration was as long as 80 μs with a current amplitude of several tens of A (see Fig. 9a). Moreover, in Figure 9b we present typical waveforms of the discharge current and the discharge voltage which were obtained in a millisecond time scale of the HC high-current discharge. The latter result gives one the hope of obtaining high-current low-pressure HC discharge, may be even in a dc mode of the HC operation.

The HC discharge with current amplitude of several hundreds Amperes cannot be self-sustained in a small size HC and pressure of $10^{-2} - 10^{-3}$ Pa. Thus, it is clear that the FPS should play a key role not only in ignition but also in sustaining of the HC discharge. Therefore we carried out measurements of the current flowing from the FPS to the cathode by a Rogowsky coil. These measurements showed that $\sim$85% of the HC discharge current is flowing from the FPS (see Fig. 10), *i.e.* a major part of the electrons is emitted from the FPS. This means that the surface area of the cathode walls does not limit the discharge current. This allowed us to decrease the HC diameter from 240 mm to 180 mm without any difference in the electrical parameters of the HC discharge. We also decreased the length of the HC. In this case, beginning with a length of 11 cm the HC discharge started only at $I_{HC} \leq 800$ A and with a 5 cm length the discharge was obtained only for $I_{HC} \leq 350$ A (see Fig. 11). At present we do not have enough experimental data to explain the obtained decrease in the threshold amplitude of the HC discharge current, and additional experiments are required. Thus, this set of experiments showed that

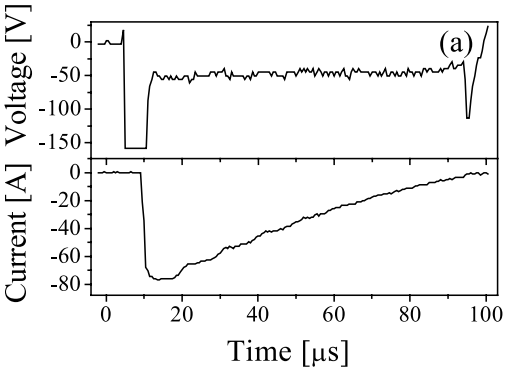

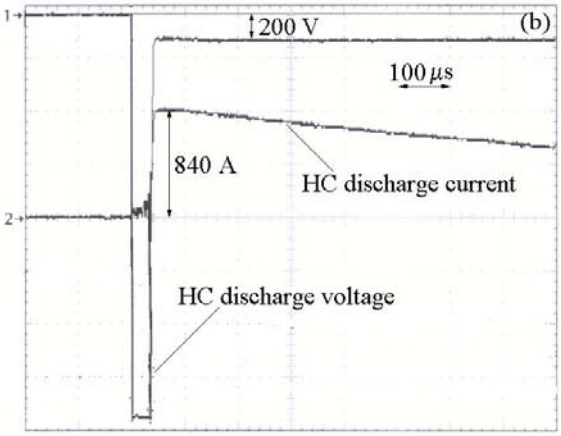

Fig. 9. Typical waveforms of the HC discharge voltage and discharge current. (a) HC with 35 cm^2 FPS and with limiting resistor in the circuit of PFN1; (b) HC with 35 cm^2 FPS supplied by a millisecond power supply.

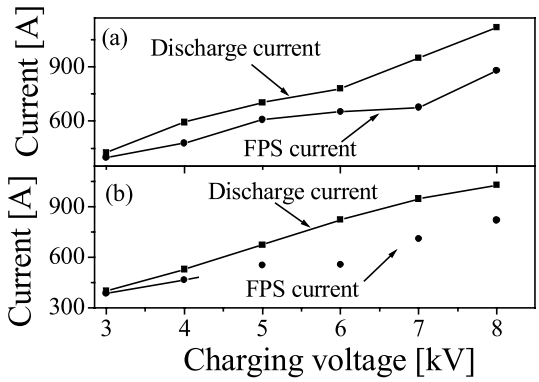

Fig. 10. Dependences of the HC discharge current amplitude and the FPS current amplitude on the charging voltage of the HC power supply for (a) 24.6 diameter HC, and (b) 18 cm diameter HC; 35 cm^2 FPS.

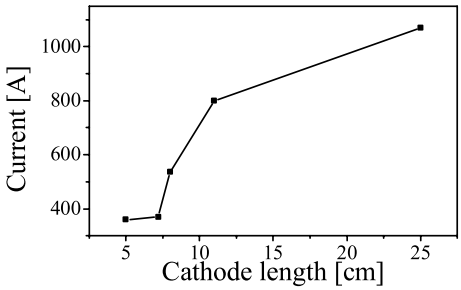

Fig. 11. Dependence of the HC discharge current on the length of the 24.6 cm diameter HC; 35 cm^2 FPS.

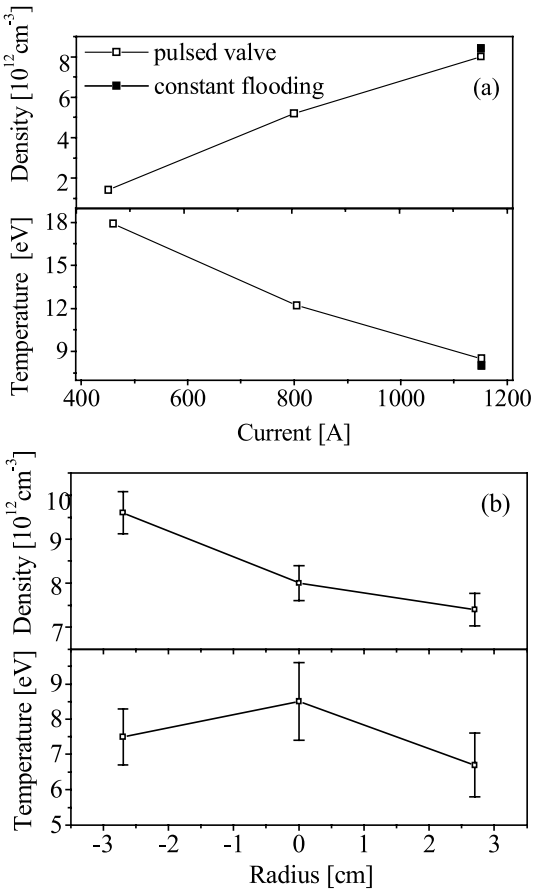

Fig. 12. (a) Dependences of the electron plasma density and temperature on the HC discharge current amplitude; (b) radial dependences of the electron plasma density and temperature. $P = 10^{-2}$ Pa with pulsed valve; $P = 2.4 \times 10^{-2}$ Pa with constant flooding; 35 cm^2 FPS.

reducing the HC surface area by almost ten times leads to only a 2.5 times decrease in $I_{\rm HC}$. Also, these measurements evidently showed the possibility of designing a compact high-current low-pressure HC electron source.

The parameters of the HC discharge plasma (plasma density and temperature) were estimated from the data obtained by double floating probe measurements [19]. In Figure 12a we present the dependence of the calculated plasma density and temperature on the amplitude of the discharge current for the case of the 35 cm^2 FPS. One can see that in both cases of the HC operation, *i.e.* with the fast gas puff valve and with the constant gas flow, we obtained an increase in plasma density and a decrease in electron temperature with the increase in amplitude of the HC discharge current. For instance, a decrease of $I_{\rm HC}$ down to 450 A led to a decrease in the plasma density down to $\sim 2 \times 10^{12}$ cm^{-3} and to an increase in the electron temperature up to 18 eV. The radial distribution

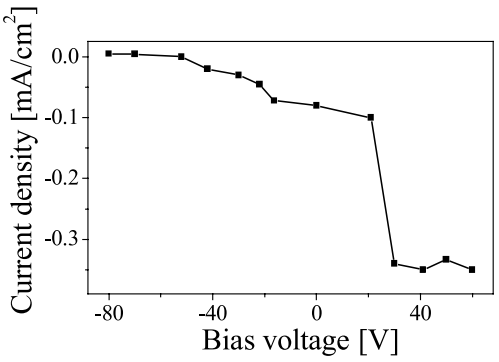

Fig. 13. Dependence of the current density collected by the CFC on the bias voltage.

of the plasma density measured at three radial positions inside the HC at a distance of 2 cm from the output grid is presented in Figure 12b. One can see satisfactory uniformity of the radial plasma density within a circle with 3 cm radius. However, at a larger radius a significant decrease of the plasma density was obtained. Namely, at a radius of 5 cm the plasma density was $\sim 2 \times 10^{12}$ cm^{-3}. This means that in the case of the 35 cm^2 FPS one obtains some constriction of the HC discharge. This is in qualitative agreement with the light emission obtained from the HC anode grid, which shows more intense light emission from the central part of the anode grid as compared with its peripheral parts. In the case of the 154 cm^2 FPS we obtained better uniformity of the plasma density radial distribution without a significant decrease in the plasma density at the peripheral parts of the HC. However, in this case the plasma density was found to be less than for the case of the 35 cm^2 FPS. Namely, for the HC discharge current amplitude in the range of 0.6–1.4 kA, the plasma density changed in the range of 4–7 $\times 10^{11}$ cm^{-3}, respectively.

In order to estimate the plasma potential we performed measurements of the energy of ions emitted from the HC plasma inside the accelerating gap. For these measurements we used a positively biased CFC with and without transverse permanent magnets. The latter were used to cut-off co-moving plasma electrons. These measurements showed that the ion energy $\leq$25 eV, which means that the HC plasma has a positive potential with respect to the output anode grid $\leq$25 V (see Fig. 13). Now, taking into account the measured HC discharge voltage of $\sim$100 V, one can estimate the cathode potential fall of $\sim$125 V. Let us note that plasma ions which are accelerated by this cathode potential fall acquire an energy of an 125 eV which is sufficient to cause a significant sputtering of the ferroelectric [20].

It was also important to know the parameters of the plasma which penetrates and fills the accelerating gap prior to the application of the accelerating pulse. These measurements performed by the biased CFC in the case of 35 cm^2 FPS showed that the ion current density is $\leq$0.1 A/cm^2 at a distance of 5 mm from the grid with a fast decrease at a further distance from the anode grid. Taking into account that the ion energy is $\sim$25 eV, one can estimate that the plasma density inside the accelerating gap does not exceed $\approx 3 \times 10^{11}$ cm^{-3} which is sufficient for space-charge neutralization of the electron beam.

3.4 Parameters of the diode and generated high-current electron beam

The HC with the incorporated 35 cm^2 area FPS was used for the generation of electron beams in a diode under an accelerating dc voltage $\leq$30 kV or a pulsed accelerating voltage $\leq$300 kV. The experiments with the dc accelerating voltage showed a HC plasma expansion inside the 5 cm width accelerating gap towards the collector [15]. Estimates showed that the obtained increase of the diode current amplitude up to 500 A corresponds to $\sim$3.5 cm expansion of the plasma inside the accelerating gap. This can be explained by an excess of the plasma thermal current density under the current density required by the space charge law.

In the case of the pulsed accelerating voltage we always obtained a plasma pre-filled mode of diode operation because the accelerating pulse was applied with a variable time delay with respect to the beginning of the HC discharge. Using the fast framing camera it was found that this mode of operation is characterized by the appearance of plasma spots at the anode grid already within a few ns after the beginning of the accelerating pulse (see Fig. 14a). This can be explained by a fast increase in the plasma positive potential due to the extraction of electrons from the plasma. The latter leads to a large potential drop in the double layer between the plasma and the HC anode grid, and consequently to the appearance of explosive emission centers at the anode grid.

In order to decrease the plasma density inside the accelerating gap prior to the beginning of the accelerating pulse and thus, to avoid the explosive plasma formation, an HC anode grid with a 20% transparency was used. Because of the restriction in the plasma emission capability the amplitude of the electron beam decreased to $\sim$300 A which is less than its space-charge limited value, and the current amplitude was almost constant during the accelerating pulse (see Fig. 15a). A larger amplitude of diode current without formation of explosive emission spots at the HC anode grid was obtained with the 154 cm^2 area FPS and an HC with a length of 11 cm. With this FPS, an electron beam generation with current amplitude of 1.6 kA was successfully demonstrated (see Fig. 15a) [15]. We calculated the diode impedance, power and energy for these two cases (see Fig. 15b). One can see that even for the case of 154 cm^2 FPS one obtains an increase in the impedance that is typical for a plasma pre-filled mode of the diode operation. Also, taking into account that the total energy stored in the PFN3 was $\sim$150 J one can conclude that about 30% efficiency of the stored energy is transferred to the kinetic energy of the electron beam.

The current density cross-sectional distribution was obtained by X-ray imaging of the collector (see Sect. 2). It was found that for the 35 cm^2 FPS the X-ray image has a bright maximum with a radius of $\sim$3 cm (see Fig. 14c)

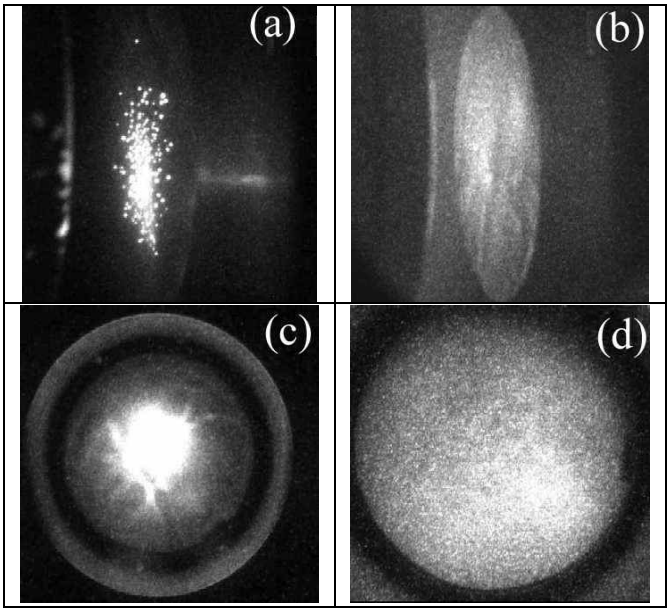

Fig. 14. (a) Typical framing photograph of the light emission from the HC anode grid during the accelerating pulse; 35 cm^2 FPS. $I_{\rm HC} \approx 1000$ A, $I_d = 1.4$ kA, $\varphi_{ac} = 120$ kV, $d_{ac} = 4$ cm. Frame duration 10 ns. (b) Typical framing photograph of the light emission from the HC anode grid during the accelerating pulse. 154 cm^2 FPS. $I_{\rm HC} \approx 1200$ A, $I_d = 1.6$ kA, $\varphi_{ac} = 100$ kV, $d_{ac} = 4$ cm. Typical X-ray images of the electron beam in the case of (c) 35 cm^2 FPS and (d) 154 cm^2 FPS. Frame duration 100 ns.

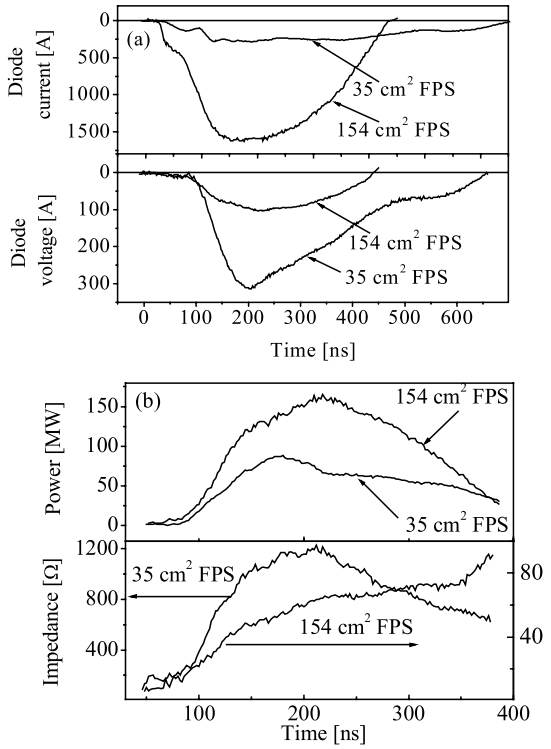

Fig. 15. (a) Typical waveforms of the diode current and voltage obtained with a 35 cm^2 FPS ($I_{\rm HC} \approx 550$ A) and a 154 cm^2 FPS ($I_{\rm HC} \approx 1200$ A), $d_{ac} = 4$ cm; (b) calculated diode impedance and power for the diode operation presented in (a).

which agrees with plasma density distribution measurements (see Sect. 3.3). In the case of the 154 cm^2 FPS a more uniform light emission from the plasma located at the HC anode grid as well as more uniform X-ray images of the collector were obtained (see Figs. 14b and 14d). Let us note that the framing photographs obtained with H_α and H_β filters showed the absence of the light emission of excited hydrogen. The latter indicates on the absence of hot plasma spots formation during high-current HC discharge. This can be explained by the decrease in the HC plasma density for the larger area PFS. Let us note that in our experiments we were restricted in the amplitude of the generated electron beam current by the impedance of the PFN generator and not by the emission capability of the plasma. Finally, in the present experiments we did not perform a special test for the lifetime of the HC with an incorporated FPS. However, we can state that we did not obtain any visible damage of the front surface FPS even after several thousand shots.

4 Discussion

The experimental data allow us to assume the following scenario for the HC operation. It was shown that ≈85% of the total discharge current is emitted by the FPS. The latter strongly indicates that the current carrying electrons are emitted mainly from the FPS surface plasma. The obtained framing photographs also showed that during the HC discharge there is a very bright light emission from the surface of the FPS. This allows us to speculate that during the HC discharge there is additional plasma formation in the vicinity of the ferroelectric surface. This additional plasma could be formed due to ionization of the adsorbed surface neutral atoms and molecules [21] by ions emitted from the HC positively charged plasma. Indeed, it was measured that the energy of the ions emitted from the HC is ≤25 eV which can only be realized in the case when the plasma has a positive potential with respect to the cathode. Therefore, these ions are accelerated up to ∼125 eV towards the FPS front surface and could cause efficient sputtering and ionization of surface atoms and molecules, resulting in a constant supply of atoms and molecules. Additional plasma formation may be also occurred by the charging of the front surface of the ferroelectric by plasma ions which can cause surface discharges. It is understood that additional measurements (in particular spectroscopic measurements) are strongly required in order to characterize this surface plasma.

Measurements of the HC plasma density at $I_{\rm HC} \approx 1.4$ kA showed that while in the case of the 35 cm^2 FPS $n_e \leq 8 \times 10^{12}$ cm^{-3}, in the case of the 154 cm^2 FPS $n_e \leq 7 \times 10^{11}$ cm^{-3}. These measurements showed a relatively high ionization degree of the gas inside the HC (one can estimate roughly the average ionization degree as 20%) which can be achieved only in the case of the

existence of the HC effect, *i.e.* electron oscillations inside the cathode cavity. These oscillations lead to a longer lifetime of electrons in the HC cavity and to an increase of ionizing collisions before electrons leave the plasma through the HC anode grid.

Thus one can conclude that the FPS plays the role of an efficient electron source. Electrons are extracted from the ferroelectric surface and accelerated by the cathode potential fall in the double sheath which exists between the FPS dense surface plasma and the relatively dilute HC plasma. These electrons conduct a major part of the HC discharge current. Also, these electrons can ionize gas atoms and molecules in the cathode cavity where they are captured in the positive plasma potential well. The discharge current arrives at the HC anode by the flow of plasma electrons whose energy is enough to affect penetration through the plasma potential barrier to reach the anode. Let us estimate the width of the double layer between the FPS surface plasma and the HC plasma. Taking into account that a bi-polar electron-ion current flows in this double layer one can express the ion current density as [22]: $j_i = 1.86 \times 50(m_p/M_i)^{1/2}\varphi_c^{3/2}d_c^{-2}$, where $\varphi_c \approx 1.3 \times 10^{-4}$ MV is the cathode potential fall, d_c is the width of the cathode double layer, and m_p, M_i are the proton and the ion masses. In our case, for N^+ ions one obtains $(m_p/M_i)^{1/2} \approx 0.27$. On the other hand the maximal amplitude of the ion current density is limited by the ion thermal current [1]: $j_{i\mathrm{th}} \approx 0.25 n_i e(kT_e/M_i)^{1/2}$, where $n_i \approx 8 \times 10^{12}$ cm^{-3} is the ion plasma density. Taking into account that the measured plasma electron temperature T_e does not exceed $\sim$8 eV and assuming that the ions are singly ionized, one can estimate $j_{i\mathrm{th}} \approx 0.2$ A/cm^2. Now, one can further estimate the width of the cathode double layer as: $d_c = (1.86 \times 50 \times 0.267\varphi_c^{3/2} j_{i\mathrm{th}})^{1/2} \approx 1.25 \times 10^{-2}$ cm and the electron plasma current density emitted from the FPS as: $j_{e\mathrm{FPS}} \approx 1.86 \times 2.2 \times 10^3 \varphi_c^{3/2} d_c^{-2} \approx 31.5$ A/cm^2. Taking into account that the area of the FPS plasma is around 35 cm^2 one obtains the total amplitude of the electron beam current as almost 1100 A. This is in a good agreement with the obtained experimental data. Indeed, we measured 1020 A for the FPS current when the HC discharge current amplitude was 1200 A. Here we neglected the ion current towards the FPS because its amplitude does not exceed 15 A. Thus, there is a very powerful electron beam which should be sufficient to sustain continuous formation of dense plasma in the HC cavity by ionization of gas atoms and molecules. Indeed, the electron beam power can be estimated as 0.13 MW that is significantly larger than the power of the thermionic cathode used in reference [13]. The obtained results also explain why we did not observe a significant difference in the HC discharge current when the cathode wall area was decreased by almost 10 times. Indeed, in the case when the FPS serves as an efficient source of electrons, there is no need for secondary electrons emitted from the cathode walls as a result of ions bombardment.

Now let us consider the current towards the HC anode grid. One can write that $I_{\mathrm{HC}} = I_e - I_i$, where $I_i = j_{i\mathrm{th}} S_A$, S_A is the anode area, $j_{i\mathrm{th}}$ is the ion current, $I_e = I_{ef} + I_{pl} = S_{\mathrm{FPS}} j^*_{e\mathrm{FPS}} + S_A j_e$ is the electron current, and S_{FPS} is the FPS area. The latter can be considered as the sum of the current of the fast electrons $S_{\mathrm{FPS}} j^*_{e\mathrm{FPS}}$ emitted from the FPS plasma which pass through the HC cavity without any significant energy loss, and of the current of plasma electrons $I_{pl} = S_A j_e$ which have enough energy to penetrate the HC plasma potential barrier, $j_e = j_{e\mathrm{th}} \exp(-e\varphi_{pl}/kT_e)$. In our case the thermal current density of plasma electrons is: $j_{e\mathrm{th}} = n_e e V_{\mathrm{th}} = 230$ A/cm^2. Thus, one can estimate $j_e \approx 10$ A/cm^2 which yields the total current of electrons penetrating the potential barrier of the plasma as $\sim$1130 A. This estimate shows that the major input to the anode current is thermal plasma electrons penetrating through the plasma potential barrier. Here we neglected once more the ion current which does not exceed several tens of A. Also, this estimate shows that the input of fast electrons to the anode current should be much smaller compared with the thermal plasma electrons. This is in agreement with conclusions obtained in references [5,11]. Namely, fast electrons emitted from the cathode (in our case, from the FPS), being trapped inside the potential well, undergo oscillations and dissipate their energy in the HC plasma by collisions and ionizations with plasma charged particles and atoms, respectively. Concerning the energetic electrons emitted from the dense FPS plasma, we can only speculate that they are trapped inside the plasma potential well due to fast energy dissipation inside the plasma. This can be explained, for instance, by development of Langmuir instability [23].

The present experimental results and their analysis show an important new application of the FPS. Namely, incorporation of the FPS inside the HC allows one to ignite and to sustain low-pressure high-current discharge while keeping a small size of the HC. It was shown that the FPS ignites the main HC discharge due to injection of relatively dense flows of electrons and ions. Further, the development of the HC discharge is accompanied by the formation of additional dense plasma at the vicinity of the FPS surface. This plasma serves as a powerful source of current carrying electrons which are accelerated in the double layer between this dense plasma and the HC plasma. In our future experiments we are planning to study the mechanism of this plasma formation and its parameters by spectroscopic non-disturbing methods.

In addition it was shown that the HC plasma is characterized by a positive potential of 15 eV, density up to 8×10^{12} cm^{-3} and electron temperature of 8 eV. A relatively low plasma potential and relatively large plasma density result in fast plasma expansion towards the accelerating gap. This leads to plasma pre-filled mode of the diode operation. In order to avoid this disadvantage we are planning experiments with an HC control biased grid which should prevent electron flow towards the accelerating gap during the HC discharge.

The authors are indebted to E.M. Oks and V.I. Gushenets for fruitful discussions. They are also grateful to A. Sayapin and K. Chirko for technical assistance.

References

1. J. Reece Roth, *Industrial Plasma Engineering* (Institute of Physics Publishing, Bristol, UK, 1995)
2. A.S. Gilmour Jr, *Microwave Tubes* (Artech House, Norwood, MA, 1986)
3. G.A. Mesyats, *Explosive Electron Emission* (URO, Ekaterinburg, 1998)
4. G. Rosenman, D. Shur, Ya.E. Krasik, A. Dunaevsky, J. Appl. Phys. **88**, 6109 (2000), and references therein
5. E.M. Oks, P.M. Schanin, Phys. Plasmas **6**, 1649 (1999)
6. Ya.E. Krasik, A. Dunaevsky, A. Krokhmal, J. Felsteiner, A.V. Gunin, I.V. Pegel, S.D. Korovin, J. Appl. Phys. **89**, 2379 (2001), and references therein
7. E. Garate, R. McWilliams, D. Voss, A. Lovesee, K. Hendricks, T. Spencer, M.C. Clark, A. Fisher, Rev. Sci. Instr. **66**, 2528 (1995)
8. D. Shiffler, M. Ruebush, D. Zagar, M. LaCour, M. Sena, K. Golby, M. Haworth, R. Umstadt, J. Appl. Phys. **91**, 5599 (2002), and references therein
9. A. Dunaevsky, Ya.E. Krasik, J. Felsteiner, A. Sternlieb, J. Appl. Phys. **90**, 3689 (2001)
10. A. Dunaevsky, Ya.E. Krasik, J. Felsteiner, J. Appl. Phys. **91**, 975 (2002)
11. E.M. Oks, Plasma Sources Sci. Techn. **1**, 249 (1992), and references therein
12. D.M. Goebel, R.W. Schumacher, R.L. Eisenhart, IEEE Trans. Plasma Sci. **26**, 354 (1998)
13. D.M. Goebel, R.M. Watkins, Rev. Sci. Instr. **71**, 388 (2000)
14. J.Z. Gleizer, A. Krokhmal, Ya.E. Krasik, J. Felsteiner, J. Appl. Phys. **91**, 3431 (2002)
15. A. Krokhmal, J.Z. Gleizer, Ya.E. Krasik, J. Felsteiner, Appl. Phys. Lett. **81**, 4341 (2002)
16. Ya.E. Krasik, A. Dunaevsky, J. Felsteiner, J. Appl. Phys. **85**, 7946 (1999)
17. A. Dunaevsky, Ya.E. Krasik, J. Felsteiner, S. Dorfman, J. Appl. Phys. **85**, 8464 (1999)
18. A. Dunaevsky, Ya.E. Krasik, J. Felsteiner, A. Krokhmal, J. Appl. Phys. **87**, 3270 (2000)
19. Yu.P. Raizer, *Gas Discharge Physics* (Springer-Verlag, New York, 1998)
20. M.D. Gabovich, N.V. Pleshivzev, N.N. Semashko, *Ion and atom beams for controlled thermonuclear fusion and technological purposes* (Energoatomizdat, Moscow, 1986)
21. K. Chirko, Ya.E. Krasik J. Felsteiner, J. Appl. Phys. **92**, 5691 (2002)
22. R.B. Miller, *Introduction to the Physics of Intense Charged Particle Beams* (Plenum, New York, 1982), and references therein
23. M.V. Nezlin, *Physics of Intense Beams in Plasmas* (Institute of Physics Publishing, 1993)